Computer Physics Communications 182 (2011) 232–236

Contents lists available at ScienceDirect

Computer Physics Communications

www.elsevier.com/locate/cpc

The evolution of solitons in coupled resonator optical waveguides and photonic-crystal waveguides

Chih-Hsien Huang [a,c], Jing-Nuo Wu [a,b], Szu-Cheng Cheng [b], Wen-Feng Hsieh [a,c,*]

[a] Department of Photonics & Institute of Electro-Optical Engineering, National Chiao Tung University, 1001 Tahsueh Rd., Hsinchu 30050, Taiwan
[b] Department of Physics, Chinese Culture University, Yang-Ming Shan, Taipei 111, Taiwan
[c] Institute of Electro-Optical Science and Engineering, National Cheng Kung University, No. 1, University Rd., Tainan City 701, Taiwan

ARTICLE INFO

Article history:
Received 22 February 2010
Accepted 27 May 2010
Available online 4 June 2010

Keywords:
Dynamics of nonlinear optical systems
Optical solitons
Waveguides

ABSTRACT

We successfully used the tight binding theory to derive the extended discrete nonlinear Schrödinger equation to describe the soliton propagation and to obtain the soliton propagation criteria (SPC) in the nonlinear photonic-crystal waveguides (PCWs) and coupled resonant optical waveguides (CROWs) containing Kerr media. From these criteria, we obtain the soliton-propagating region of CROWs in different numbers of separated rods and strengths of self-phase modulation (SPM). The defined soliton-propagating regions coincide with the regions of modulation instability in the CROWs. In the PCWs, the positive Kerr coefficient medium needs to be added to support the pulse propagation in low frequency or low wave vector region of the dispersion curve; while negative Kerr effect is for high frequency case. Due to the linear combination of various cosine harmonic functions in the dispersion relations of both CROWs and PCWs, the pulse broadening which is mainly caused by the third-order dispersion at SPC is the lowest at the boundary of dispersion curves. However, due to the different magnitudes of coupling coefficients in CROWs and PCWs, the group velocity, dispersion and strength of SPM in CROWs are all smaller than those in PCWs.

1. Introduction

Photonic crystal waveguides (PCWs) [1] are the optical devices carved from perfect photonic crystals (PCs) by sequentially modifying a linearly unit cells; on the other hand, the coupled resonator optical waveguides (CROWs) [2] are created by arranging the cavities, made of point defects, periodically. Light that propagates in either PCW or CROW with a frequency within the band gap of the crystal is confined to the defects, and can be conducted along the defects with a very low loss even through a sharp bend [3–5]. Several simulation methods such as the plane-wave-expansion method (PWEM) [6,7] and finite-difference-time-domain (FDTD) [8,9] method were usually used to design the waveguides with variety of functions, but they cannot provide an efficient and analytic method for understanding the physical properties of the waveguides. Therefore, the tight-binding theory (TBT) is widely used to analytically study the electromagnetic (EM) wave propagation in linear or nonlinear waveguides [10–15].

The amplitude evolution of the electric field in the nonlinear CROWs containing Kerr media, in which the refractive indices are proportional to the intensity of the EM wave, often leads to the discrete nonlinear Schrödinger equation (DNLSE) derived by the TBT [16,17]. By solving the DNLSE under long-wavelength approximation this equation reduces to a nonlinear Schrödinger equation (NLSE). Spatiotemporal discrete solitons can propagate undistorted along the defects by balancing the effects of discrete lattice dispersion with material nonlinearity [17]. However, as the pulse becomes narrow, the long-wavelength approximation will be broken and the high-order dispersions should be considered [16]. The more general criteria for solitons propagation in different structures of CROWs, e.g., different numbers of separation rods between two cavities or different pulse widths, are still leaking.

In the PCWs, however, the defect rods are so close that the next nearest-neighbor coupling cannot be neglected [12]. The governed equation of motion is termed the extended discrete nonlinear Schrödinger equation (EDNLSE) to distinguish the DNLSE in the CROWs in which only the nearest-neighbor coupling coefficient is considered. There are rare reports on pulse propagation in nonlinear PCWs using the TBT but the Green-function approach [18–20]. Although the equations obtained from these two approaches are quite similar [21], it still lacks on the research about the dynamic or criteria of soliton propagation in the PCWs especially under the high-order influence. Therefore, it is needed to take the advanced

* Corresponding author at: Department of Photonics & Institute of Electro-Optical Engineering, National Chiao Tung University, 1001 Tahsueh Rd., Hsinchu 30050, Taiwan.
E-mail addresses: scheng@faculty.pccu.edu.tw (S.-C. Cheng), wfhsieh@mail.nctu.edu.tw (W.-F. Hsieh).

0010-4655/$ – see front matter
doi:10.1016/j.cpc.2010.05.009

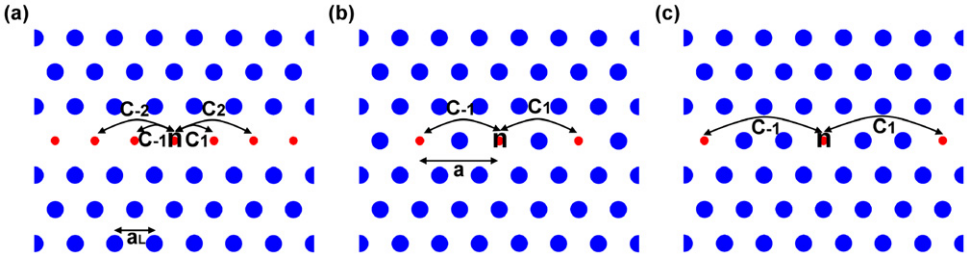

Fig. 1. The structures of (a) a PCW, (b) a CROW with one separation rod, and (c) a CROW with two separation rods. Here a is the length of successive defect points and a_L is the lattice constant of a PC.

discussion about criteria of solitons propagation of different kinds of CROWs and PCWs, and to derive the EDNLSE for describing the dynamic properties or the high-order dispersion of solitons with different nonlinear strengths and pulse widths. It can provide a physical concept to design PCWs or CROWs allowing pulse propagation with low pulse broadening.

We will first use the TBT to derive the EDNLSE in this paper. Second, by considering the Taylor expansion of the pulse envelope, the soliton criteria in different kinds of CROWs and PCWs are derived and discussed. Third, the pulse broadening of soliton propagation at the soliton criteria is discussed. Finally, by using the fourth-order Runge–Kutta method, a CROW and a PCW with triangular lattices were proposed to demonstrate the soliton propagation. We found the simulation results can be well explained by the analytic analyses.

2. Theory

To describe the solitons propagating in CROWs or PCWs, we consider a PC with the lattice constant a_L and the waveguides consisting of a periodic sequence of identical single-mode defects. The distance between successive defect points or cavities is a, and the Kerr media is localized in the defect regions as shown in Fig. 1. Assuming the eigenfrequency of the isolated point defect is ω_0, we can express the electric and magnetic fields in the waveguides as the linear combination of the isolated cavity mode $\mathbf{E}_0$ and $\mathbf{H}_0$, i.e., $\mathbf{E}'_0(\mathbf{r},t)=\sum b_m(t)\mathbf{E}_{0m}$ and $\mathbf{H}'_0(\mathbf{r},t)=\sum b_m(t)\mathbf{H}_{0m}$, where $\mathbf{E}_{0m}=\mathbf{E}_0(\mathbf{r}-ma)$ and $\mathbf{H}_{0m}=\mathbf{H}_0(\mathbf{r}-ma)$. Under the tight-binding approximation, we can get the EDNLSE as [17]

$$i\frac{db_n}{dt}+(-\omega_0+c_0)b_n+\sum_{m=1}^{M}c_m(b_{n+m}+b_{n-m})+\gamma|b_n|^2b_n=0. \tag{1}$$

The upper limits M of summations representing the considered maximal coupling neighbors for Eqs. (1) and (4) to describe the EM wave propagation should be 1 in the CROWs but 2 in the PCWs. Here the linear coupling coefficient c_m is defined as

$$c_m=\frac{\omega_0\iiint d\upsilon\,\Delta\varepsilon E_{0n}\cdot E_{0n+m}}{\iiint d\upsilon\,(\mu_0|H_{0n}|^2+\varepsilon|E_{0n}|^2)} \tag{2}$$

with $\Delta\varepsilon(\mathbf{r})=\varepsilon'(\mathbf{r})-\varepsilon(\mathbf{r})$ being the difference of unperturbed and perturbed total permittivity and c_0 representing a small shift in the eigen frequency ω_0 that arises from present of the neighbor defects or cavities. The self-phase modulation (SPM) strength γ is given by

$$\gamma=\frac{2n_0n_2\varepsilon_0\omega_0\iiint d\upsilon\,|E_{0n}|^4}{\iiint d\upsilon\,(\mu_0|H_{0n}|^2+\varepsilon|E_{0n}|^2)} \tag{3}$$

with n_2 being the Kerr coefficient. Let the plane wave with frequency ω, propagation wavevector k, and amplitude ϕ in site n as $b_n=\phi\exp(inka-i\omega t)$ be the solution of Eq. (1). The dispersion relation of the nonlinear PCW or CROW can be derived as

$$\begin{aligned}\omega(ka)&=\omega_0-c_0-\sum_{m=1}^{M}2c_m\cos(mka)-\gamma|\phi|^2\\&=\omega'(ka)-\gamma|\phi|^2.\end{aligned} \tag{4}$$

Here, ω' is the frequency of the PCWs without nonlinear media and the Kerr media make the dispersion curve a constant frequency shift in all wave vectors [22].

In order to get the soliton solution and to give the advanced analysis of high-order dispersion as pulse propagating, we let $x=na$ and $b_n=\phi e^{i(kx-\omega' t)}$. Taking the Taylor expansion of ϕ, [16]

$$\boldsymbol{\phi}(\boldsymbol{x}+\boldsymbol{a})=\boldsymbol{\phi}+\sum_{\boldsymbol{n}=1}\frac{\boldsymbol{a}^{\boldsymbol{n}}}{\boldsymbol{n}!}\frac{\partial^{\boldsymbol{n}}\boldsymbol{\phi}}{\partial\boldsymbol{x}^{\boldsymbol{n}}}, \tag{5}$$

Eq. (1) can be written as an NLSE:

$$\boldsymbol{i}\frac{\partial\boldsymbol{\phi}}{\partial\boldsymbol{t}}-\sum_{\boldsymbol{n}=1}\frac{(-\boldsymbol{i})^{\boldsymbol{n}}}{\boldsymbol{n}!}\boldsymbol{\beta}_{\boldsymbol{n}}\frac{\partial^{\boldsymbol{n}}\boldsymbol{\phi}}{\partial\boldsymbol{x}^{\boldsymbol{n}}}+\boldsymbol{\gamma}|\boldsymbol{\phi}|^2\boldsymbol{\phi}=0. \tag{6}$$

The dispersion coefficients, β_n, equal to $\partial^n\omega(k)/\partial k^n$ or

$$\boldsymbol{\beta}_{2\boldsymbol{n}-1}=2\boldsymbol{a}^{2\boldsymbol{n}-1}(-1)^{\boldsymbol{n}+1}\sum_{\boldsymbol{m}=1}\boldsymbol{m}^{2\boldsymbol{n}-1}\boldsymbol{c}_{\boldsymbol{m}}\sin(\boldsymbol{mka}), \tag{7}$$

$$\boldsymbol{\beta}_{2\boldsymbol{n}}=2\boldsymbol{a}^{2\boldsymbol{n}}(-1)^{\boldsymbol{n}+1}\sum_{\boldsymbol{m}=1}\boldsymbol{m}^{2\boldsymbol{n}}\boldsymbol{c}_{\boldsymbol{m}}\cos(\boldsymbol{mka}). \tag{8}$$

Therefore, the angular frequency of the waveguides can also be expressed as the Taylor's expansion sum of dispersion coefficients, i.e.,

$$\boldsymbol{\omega}(\boldsymbol{k})=\boldsymbol{\omega}_0+\boldsymbol{\beta}_1\Delta\boldsymbol{k}+\boldsymbol{\beta}_2(\Delta\boldsymbol{k})^2/2!+\boldsymbol{\beta}_3(\Delta\boldsymbol{k})^3/3!+\cdots, \tag{9}$$

where β_1 is the group velocity (v_g) of the solitons in these waveguides as the high-order terms are neglected. When the variation of the pulse amplitude is smooth enough, i.e., $\boldsymbol{\beta}_n(\Delta\boldsymbol{k})^{\boldsymbol{n}}/\boldsymbol{n}!\approx 0$ or $\boldsymbol{\beta}_{\boldsymbol{n}}\frac{\partial^{\boldsymbol{n}}\boldsymbol{\phi}}{\partial\boldsymbol{x}^{\boldsymbol{n}}}\approx 0$ for $n>2$, Eq. (6) has a soliton solution as

$$\boldsymbol{b}=\boldsymbol{\phi}\,\mathrm{sech}\left(\frac{\boldsymbol{x}-\boldsymbol{\beta}_1\boldsymbol{t}}{\boldsymbol{x}_0}\right)\boldsymbol{e}^{\boldsymbol{i}(\boldsymbol{kx}-\boldsymbol{\omega t})}. \tag{10}$$

The criterion to support a soliton propagation is thus $\boldsymbol{\gamma\phi}^2=\boldsymbol{\beta}_2/\boldsymbol{x}_0^2$ or

$$\boldsymbol{\gamma\phi}^2=2\boldsymbol{a}^2\left(\boldsymbol{c}_1\cos(\boldsymbol{ka})+4\boldsymbol{c}_2\cos(2\boldsymbol{ka})+9\boldsymbol{c}_3\cos(3\boldsymbol{ka})+\cdots\right)/\boldsymbol{x}_0^2. \tag{11}$$

From Eq. (10), the dispersion relation of the solitons is the same as a plane wave incident into the nonlinear waveguides. The relationship between x_0 and ϕ is determined by β_2 and γ (n_2 or $\chi^{(3)}$). The sign of β_2 and γ must be the same to support a soliton propagation and SPM strength (γ_s) is $\boldsymbol{\beta}_2/(\boldsymbol{x}_0^2\boldsymbol{\phi}^2)$.

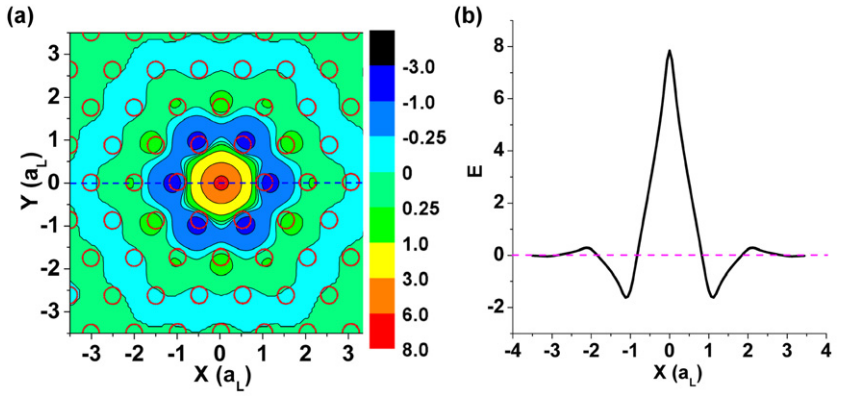

Fig. 2. (a) The electric field distribution (E_z) of a point defect mode simulated by the plane wave expansion method in the triangular lattice with the dielectric constant, radii of dielectric rods and the radius of the defect rods being 12, $0.2a_L$ and $0.1a_L$ for a frequency (f) $= 0.333c/a_L$. (b) The field distribution of the blue dash line in (a). (For interpretation of the references to color in this figure legend, the reader is referred to the web version of this article.)

Table 1
The soliton propagation region of the CROW with different separation rods.

Separation rods	Sign of c_1	Sign of $n_2(\gamma)$	Region (ka)
Odd	−	+	$> \pi/2$
		−	$< \pi/2$
Even	+	+	$< \pi/2$
		−	$> \pi/2$

3. Soliton propagation condition

In this section, we will further discuss the soliton-propagation region (in k or ω) in different structures, e.g., PCWs and CROWs with different separated rods as shown in Fig. 1 containing Kerr media with different signs and Kerr coefficients. The electric field distribution (E_z) of a single point defect simulated by the PWEM in the triangular lattice with the dielectric constant, radii of dielectric rods and the radius (r_d) of the defect rods being 12, $0.2a_L$ and $0.1a_L$ for the frequency $f = 0.333c/a_L$ is shown in Fig. 2. The field profile along the blue dash line in Fig. 2(a) is plotted in Fig. 2(b); it has the opposite sign when extending to the odd nearest-neighbor rod(s) ($\mathbf{E}_0(0,0) * \mathbf{E}_0(xa,0) < 0$, $x = 1, 3, 5, \ldots$) and has the same sign when extending to the even nearest-neighbor rods. To maintain a single mode propagating in the waveguides, the radii or the refraction indices of the rods in the waveguides are reduced, therefore $\Delta\varepsilon$ are negative in the following discussion. Since the electric field is mainly localized around the dielectric rods of the waveguides, we can use the maximum values to replace the integral values for a simple estimation of Eq. (2). Therefore, c_1 is positive in even-separated-rod CROWs [23], in which $\mathbf{E}_0(0,0) * \mathbf{E}_0(xa,0) < 0$, $x = 1, 3$; c_1 is negative in odd-separated-rod CROWs. In the PCWs, c_1 and c_3 are positive and c_2 and c_4 are negative.

In the CROWs, c_2 is two orders of magnitude smaller than c_1, so c_2 can be neglected in considering β_2 and the soliton propagation criterion (SPC) in Eq. (11) can be further reduced to $\boldsymbol{x}_0^2/\boldsymbol{a}^2 = 2\boldsymbol{c}_1\cos(\boldsymbol{ka})/(\boldsymbol{\gamma\phi}^2)$. In the CROWs with even separated rods, c_1 is positive so γ should be positive in order to achieve the SPC when $ka < \pi/2$ and should be negative as $ka > \pi/2$; however, in odd separated rod(s), c_1 is negative so γ should be negative (positive) when $ka < \pi/2$ ($ka > \pi/2$) to reach the SPC that corresponds to the modulation instability in these nonlinear waveguides [23] and the Kerr media should switch their signs when ka crosses $\pi/2$. The soliton propagation region of the CROWs is shown in Table 1. In PCWs, c_1 is positive and c_2 is negative with its value being an order of magnitude smaller than c_1 [23]. Therefore, positive Kerr media should be put in the waveguides as a low wave vector or low frequency EM wave is incident, and vice versa. When the coupling coefficients c_n ($n > 2$) are neglected for a simply estimation, Eq. (11) can be written as $\cos(ka) = -4|c_2/c_1|$ if $\gamma = 0$. Therefore, the border of switching sign of Kerr medium for soliton propagation in PCWs occurs at $ka > \pi/2$. However, if the dielectric defect is used, in which $\Delta\varepsilon > 0$, the signs of c's should be changed and the type of Kerr media would also be changed accordingly.

4. High-order dispersion effect

To estimate the influences of high-order linear dispersion which makes the pulse broadening, we took the Fourier transform of the soliton solution, $\mathrm{sech}(x/x_0)$, and calculated the standard deviation of k's distribution as $\Delta k = 1/x_0$. Taking derivative of Eq. (9) with respect to k, the group velocity can be expressed as

$$\partial\boldsymbol{\omega}/\partial\boldsymbol{k} = \boldsymbol{\beta}_1 + \boldsymbol{\beta}_2(\Delta\boldsymbol{k}) + \boldsymbol{\beta}_3(\Delta\boldsymbol{k})^2/2! + \boldsymbol{\beta}_4(\Delta\boldsymbol{k})^3/3! + \cdots. \quad (12)$$

When the dispersion of β_2 is balanced by the SPM and $x_0 > a$, the pulse broadening will be mainly dominated by β_3. The group velocity dispersion (GVD) arising from β_3 is determined by $0.5\beta_3\Delta k^2 = 0.5\beta_3\Delta(1/x_0)^2$ so that it can be neglected when $0.5\beta_3\Delta k^2 t \approx 0$. Similarly, from Eq. (7),

$$\boldsymbol{\beta}_3 = -2\boldsymbol{a}^3\sum_{\boldsymbol{m}=1}\boldsymbol{m}^{2\boldsymbol{n}-1}\boldsymbol{c}_{\boldsymbol{m}}\sin(\boldsymbol{mka}), \quad (13)$$

which means the pulse broadening is minimized when $ka = 0$ or π/a no matter in CROWs or PCWs. In the CROWs, only c_1 term needs to be considered so $\boldsymbol{\beta}_3 = -2\boldsymbol{a}^3\boldsymbol{c}_1\sin(\boldsymbol{ka})$ and the largest dispersion occurs at $ka = \pi/2$. In the PCWs, c_2 term also contributes to the dispersion and has opposite sign with c_1 so the largest dispersion happens as ka exceeds $\pi/2$.

5. Simulation results and discussion

We consider triangular-lattice PCs with the dielectric constant and radius of the dielectric rods being 12 and $0.2a_L$. The radius (r_d) of the defect rods is reduced to $0.1a_L$ and the Kerr media are introduced in the defects between one separation rod to create the CROW and sequentially to create the PCW. The dispersion curves, which were simulated by the PWEM, and dispersion coefficients (β_n) of the CROW and PCW in TM polarization (the electric field parallels the rod axis) without Kerr media are shown in Fig. 3. The coupling coefficient of c_1 is -0.00652 ($2\pi c/a$) in the CROWs and c_1, c_2 and c_3 are 0.02041, -0.00205 and 0.00026 ($2\pi c/a$) in the PCWs, respectively.

Due to the magnitude of the coupling coefficient in the CROW is smaller than those in the PCW, the magnitude of the group velocity (β_1) and the higher dispersion coefficients ($\beta_{2,3,4}$) in CROWs

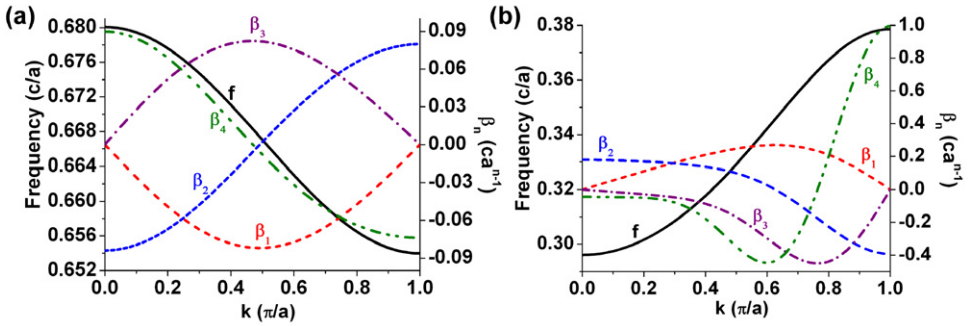

Fig. 3. The dispersion relations and dispersion coefficients of (a) a CROW with one separation rod and (b) a PCW in triangular lattices calculated by the plane wave expansion method.

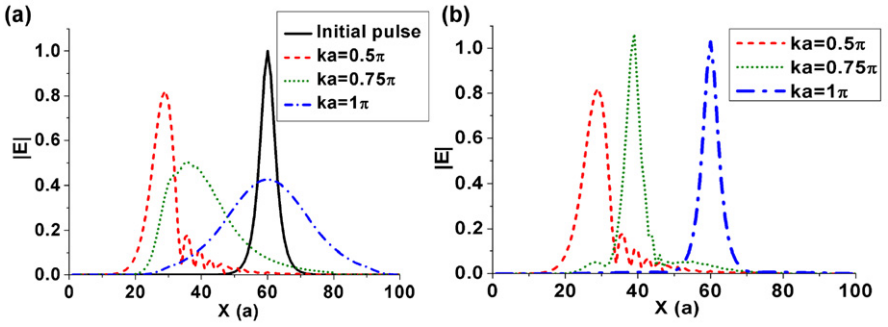

Fig. 4. The hyperbolic-secant (HS) pulse ($x_0 = 2a$) propagates in the CROWs of different wave vectors at $t = 400a/c$ (a) without Kerr medium and (b) at the soliton propagation criterion by using the fourth-order Runge–Kutta method. The black solid line in (a) is the incident pulse.

would be smaller than in PCWs. However, because the signs of $c_1's$ are different so that the EM waves in these two structures will propagate in the opposite directions. The neglected c_2 term in CROWs makes $\beta_2 \approx 0$ and the values of β_3 are almost symmetric at $ka = \pi/2$, leading to soliton propagations at k and $1-k$ (in π/a unit) would be similar if different signs of Kerr media were introduced in the defects. However, it would behave quite differently in the PCWs. The border of switching sign of Kerr medium for soliton propagation occurs at $ka > \pi/2$, and the high-order dispersion coefficients (β_3) in high k are larger than those in low k due to the negligible 2nd and 3rd next-neighbor coupling coefficients.

We will use the fourth-order Runge–Kutta method to solve Eq. (1) to simulate an initial hyperbolic-secant (HS) pulse, i.e., $\phi\,\mathrm{sech}(x/x_0)e^{ikx}$, propagating in the PCW and CROWs because the HS pulse is a soliton solution. The advantage of using this method is to directly solve Eq. (1) without the requirement of calculating the dispersion coefficients due to all order dispersions are contained in this equation. However, when the split-step Fourier method [16,24] is used to solve Eq. (6), all orders of the dispersion coefficients are required to take into consideration for short pulse. On the other hand, if a Gaussian pulse is incident into the nonlinear waveguides with the same energy of the HS pulse at the SPC with small high-order GVD, the Gaussian pulse will initially develop into HS envelope, then finally the pulse becomes broadened due to the high-order dispersions that behaves like initially launching the HS pulse into the nonlinear waveguides.

To observe the pulse broadening without Kerr media or under the SPC, where $\boldsymbol{\gamma}_s = 2\boldsymbol{c}_1 a^2 \cos(\boldsymbol{ka})/(\boldsymbol{\phi}^2 \boldsymbol{x}_0^2)$ in the CROWs with one separation rod and $\gamma_s(n_2)$ is positive as $ka > \pi/2$, we sent an HS wave with $x_0 = 2a$ into the CROWs and let it propagate $400a/c$ in different k's as shown in Fig. 4. It can be seen that the pulse spreads seriously without Kerr medium but spreads slightly or even preserve at the SPC. Because $\beta_2 = 0$ at $ka = \pi/2$, the pulse would not spread even without Kerr medium, whereas, the dispersive waves were observed at the farther distance wing with the larger x in Fig. 4(a) due to the higher-order dispersion. From Fig. 3(a) we noticed that $|\beta_2|$ is largest at $ka = \pi$ so without Kerr medium the pulse becomes the broadest shown as Fig. 4(a). At the SPC, however, β_2 can be balanced by SPM and thus the pulse is basically preserving the same shape without broadening except for the larger β_3 as ka approaches $\pi/2$. Because $\beta_3 = 0$ at $ka = 0$ or π, it makes soliton propagation almost with no dispersive waves and the pulse disperse symmetrically in the waveguides even containing no Kerr media.

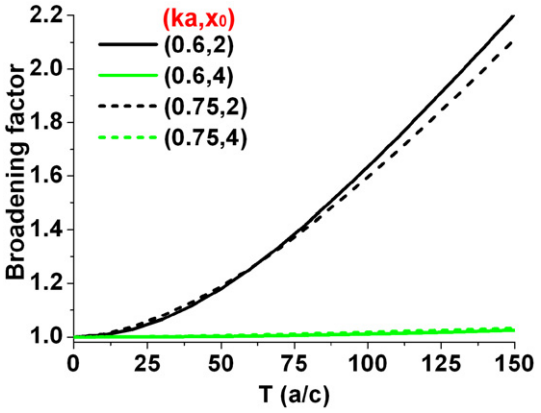

Fig. 5. The broadening factors of $ka = 0.6\pi$ and 0.75π and $x_0 = 2a$ and $4a$ of the HS envelopes at the SPC.

Now we turn to the pulse propagation in the PCWs. In order to further evaluate the degree of the pulse broadening arising from high-order dispersions, we define the broadening factor (BF) as σ/σ_0, where σ is the root-mean-square energy of output pulse and σ_0 is that of the input pulse. From the BF of PCWs at different propagating time (T) for $ka = 0.6\pi$ and 0.75π as shown in Fig. 5, the BF is proportional to T^2 as BF is small, but it is proportional

to T when BF $\gg 1$ that is similar to the Gaussian pulse propagating in the fiber [24]. Since β_3 is the largest around $ka = 0.75\pi$, BF($ka = 0.75\pi$) > BF(0.6π) initially, but becomes the other way around with BF(0.6π) > BF(0.75π) after the pulse propagates a span of $60a/c$ for $x_0 = 2a$. This is because the BF is mainly dominated by β_3 at the SPC but dominated by β_2 after having been severely distorted by β_3. When the width of pulse increases, the pulse broadening is greatly depressed.

The broadening mechanism and the formula to define the SPCs in CROWs and PCWs are similar, but the conditions γ and k to support the SPC are quite different due to differences in their coupling coefficients. Once the coupling coefficients are obtained from the PWEM, the pulse broadening and the SPC can be well analyzed by the derived equations. The simulation results obtained from the fourth-order Runge–Kutta method agree well with our analyses in both the CROWs and PCWs.

6. Conclusion

The soliton propagation in the CROWs and the PCWs containing optical Kerr media was studied using the tight-binding theory. By considering the coupling between the defects, we derived an extended discrete nonlinear Schrödinger equation to describe the wave propagation in these nonlinear waveguides. By solving this equation we obtained the criterion that supports the soliton propagation if the dispersions more than three orders can be neglected or the dispersion can be highly depressed at the criterion if the high-order dispersions cannot be neglected. The dispersion in CROWs with odd or even separated rods at different wave vectors before or after $\pi/2a$ is identified that can be balanced by positive or negative Kerr medium to support solitons propagation, separately. In PCWs with air defect, positive Kerr media must be added in the low wave vector or low frequency to support a soliton propagation and vice versa. Due to the coupling coefficients of the PCW are larger than those in the CROW the group velocity and the dispersion should also be larger in the PCWs that requires larger self phase modulation to support solitons propagation in the PCWs. When the pulse width becomes shorter, the effect of the high-order dispersion is enhanced and the third-order dispersion β_3 dominates the pulse broadening. The broadening is the lowest as the center frequency of the incident pulse located at the boundary of the dispersion curve ($ka = 0$ or π) of both PCWs and CROWS. However, the largest broadening occurs around $ka = \pi/2$ only in CROWs due the negligible next nearest-neighbor coupling coefficient c_2.

Acknowledgements

The authors would like to thank the National Science Council (NSC) of the Republic of China for partial financial support under grants NSC098-2811-E-006-074-, NSC96-2112-M-034-002-MY3, and NSC96-2628-E-009-018-MY3.

References

[1] R.D. Meade, A. Devenyi, J.D. Joannopoulos, O.L. Alerhand, D.A. Smith, K. Kash, J. Appl. Phys. 75 (1994) 4753.
[2] A. Yariv, Y. Xu, R.K. Lee, A. Scherer, Optim. Lett. 24 (1999) 711.
[3] A. Mekis, J.C. Chen, I. Kurland, S.H. Fan, P.R. Villeneuve, J.D. Joannopoulos, Phys. Rev. Lett. 77 (1996) 3787.
[4] S.H. Fan, P.R. Villeneuve, J.D. Joannopoulos, Phys. Rev. Lett. 80 (1998) 960.
[5] A. Mekis, S.H. Fan, J.D. Joannopoulos, Phys. Rev. B 58 (1998) 4809.
[6] K.M. Leung, Y.F. Liu, Phys. Rev. Lett. 65 (1990) 2646.
[7] S.G. Johnson, J.D. Joannopoulos, Opt. Express 8 (2001) 173.
[8] A. Taflove, S.C. Hagness, Computational Electrodynamics: The Finite-Difference Time-Domain Method, Artech House, Norwood, MA, 2000.
[9] H. Benisty, J. Appl. Phys. 79 (1996) 7483.
[10] T. Kamalakis, T. Sphicopoulos, IEEE J. Quantum Electron. 41 (2005) 1419.
[11] S. Mookherjea, Optim. Lett. 30 (2005) 2406.
[12] F.S.S. Chien, J.B. Tu, W.F. Hsieh, S.C. Cheng, Phys. Rev. B 75 (2007) 125113.
[13] C.H. Huang, W.F. Hsieh, S.C. Cheng, J. Opt. Soc. Amer. B 26 (2009) 203.
[14] C.H. Huang, W.F. Hsieh, S.C. Cheng, J. Opt. A, Pure Appl. Opt. 11 (2009) 015103.
[15] K. Hosomi, T. Katsuyama, IEEE J. Quantum Electron. 38 (2002) 825.
[16] I. Neokosmidis, T. Kamalakis, T. Sphicopoulos, IEEE J. Quantum Electron. 43 (2007) 560.
[17] D.N. Christodoulides, N.K. Efremidis, Optim. Lett. 27 (2002) 568.
[18] S.F. Mingaleev, Y.S. Kivshar, R.A. Sammut, Phys. Rev. E 62 (2000) 5777.
[19] S.F. Mingaleev, Y.S. Kivshar, Phys. Rev. Lett. 86 (2001) 5474.
[20] S.F. Mingaleev, A.E. Miroshnichenko, Y.S. Kivshar, K. Busch, Phys. Rev. E 74 (2006) 046603.
[21] Y.S. Kivshar, G.P. Agrawal, Optical Solitons, Academic, California, 2003.
[22] B. Maes, P. Bienstman, R. Baets, J. Opt. Soc. Amer. B 22 (2005) 613.
[23] C.H. Huang, Y.H. Lai, S.C. Cheng, W.F. Hsieh, Opt. Express 17 (2009) 1299.
[24] G.P. Agrawal, Nonlinear Fiber Optics, Academic, Burlington, MA, 2007.